Characteristic Impedance Extraction Using Calibration Comparison

S. Vandenberghe, D. Schreurs, G. Carchon,
B. Nauwelaers, W. De Raedt

ESAT TELEMIC, K.U.Leuven, B–3001 Leuven, Belgium.
IMEC, B–3001 Leuven, Belgium

Abstract

A robust line impedance identification method is presented. It determines the characteristic impedance of on-wafer TLR standards measured after an initial off-wafer LRM or TLR calibration. The only assumption made is that the obtained trans-wafer error boxes are a cascade of a symmetric probe related disturbance and a change in reference impedance. The proposed method yields an unbiased estimate of the complex characteristic impedance. Results from coplanar lines on a high resistivity silicon substrate support the made assumption.

1 Introduction

The TLR method is often the most feasible on-wafer calibration technique since it only requires two lines of a different length. A drawback is that the recovered reflection parameters are at an unknown reference impedance, set by the characteristic line impedance. An indirect determination using the propagation constant is only possible for low loss substrates[Mar91c].

Calibration comparison methods measure on-wafer TLR standards after an initial off-wafer calibration at a known reference impedance. The obtained trans-wafer error boxes are then identified with an equivalent circuit, modelling the contact geometry and substrate change, and a transformer [Car98][Will98]. This transformer accounts for the change in voltage over the virtual two port junction if the reference impedance at both ports is chosen equal. An example is the waveguide TE_{10} E-plane step junction[Col66, p. 162] where the port impedance is chosen and the modal voltage is determined from power consistency. For ideal transmission line discontinuities it is, however, more physically consistent to assume a constant voltage over the junction. This condition determines the port 2 modal voltage, reference impedance, and removes the transformer.

Both interpretations result in the same voltage normalized S-parameter values if $n = \sqrt{Z_s/Z_l}$. The normalization follows implicitely from the reciprocity condition $S_{n21} = S_{n12}$ as

$$\frac{Y_{21}}{Y_{12}} = 1 \quad \Rightarrow \quad \frac{S_{n21}}{S_{n12}} = \frac{S_{21}\sqrt{\frac{Z_{c1}}{Z_{c2}}}}{S_{12}\sqrt{\frac{Z_{c2}}{Z_{c1}}}} = 1 \tag{1}$$

shows.

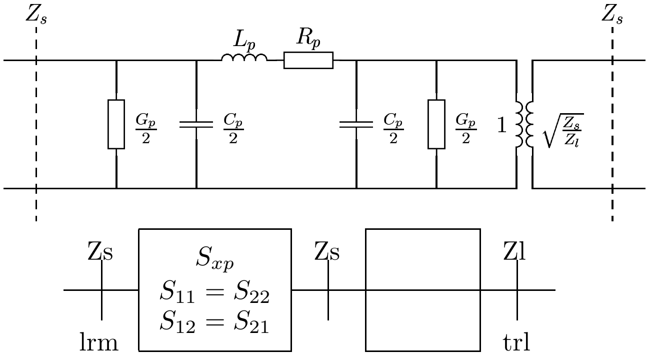

Figure 1: The error box model used for the characteristic impedance identification. Top: the equivalent circuit. Bottom: the reflection parameter based model. The S-parameter response follows from the cascade of a symmetric probe related disturbance S_{xp} and an impedance change from Z_s to Z_l.

2 Error box identification

The trans-wafer error box $x = \{a, b\}$ is modelled by a symmetric probe related disturbance S_{xp} cascaded by a change in reference impedance from Z_s to Z_l, see fig. 1. The S-parameters follow from

$$S_x^{cir} = \begin{bmatrix} S_{xp11} & S_{xp12} \\ S_{xp12} & S_{xp11} \end{bmatrix} \parallel S_z(Z_s, Z_l) \tag{2}$$

$$S_z = \frac{1}{Z_{02} + Z_{01}} \cdot \begin{bmatrix} Z_{02} - Z_{01} & 2\sqrt{Z_{01}Z_{02}} \\ 2\sqrt{Z_{01}Z_{02}} & -Z_{02} + Z_{01} \end{bmatrix} \tag{3}$$

with $S_z(Z_{01}, Z_{02})$ the response of a thru in a Z_{01}/Z_{02} environment. Equating simulated and measured S-parameters for M error boxes yields $8M$ real equations,

$$\vec{f}(\vec{x}) = \begin{bmatrix} \vdots \\ \Re(S^{cal}_{xij} - S^{cir}_{xij}) \\ \Im(S^{cal}_{xij} - S^{cir}_{xij}) \\ \vdots \end{bmatrix} = \vec{0}\,, \qquad (4)$$

of which $6M$ are independent due to reciprocity. There are $4M+2$ real unknowns since Z_s is known and Z_l is equal for all error boxes.

The linearization of $\vec{f}(\vec{x})$ in the solution reveals the sensitivity information. The jacobian is rewritten as $J = USV^T$ by the singular value decomposition, with $U = [\ldots \vec{u}_i \ldots]$ and $V = [\ldots \vec{v}_i \ldots]$ orthonormal and S a diagonal matrix of singular values s_i. From

$$\Delta\vec{f} \;\approx\; J\Delta\vec{x} = USV^T\Delta\vec{x} \qquad (5)$$

follows that the penalty $\|\Delta\vec{f}\|$ for adding $\vec{v}_i$ to the solution is given by $\|J\vec{v}_i\| = s_i$. Table 1 summarizes the results for one trans-wafer error box modelling a cpw discontinuity at 10 GHz. The estimation of Z_l is decoupled from the probe parasitics S_{xp}, which is true as long as the probe disturbance is small. The singular values indicate that $\vec{f}$ is more sensitive for the probe related unknowns. A noticeable faster convergence of the Newton-Rhapson zero solving algorithm for S_{xp}, compared to Z_l, may thus be explained.

$\vec{x} =$	$\vec{v}_1$	$\vec{v}_2$	$\vec{v}_3$	$\vec{v}_4$	$\vec{v}_5$	$\vec{v}_6$
$\Re(Z_l)$					-1.0	
$\Im(Z_l)$						-1.0
$\Re(S_{ap11})$	.17	.65	$-.72$	.20		
$\Im(S_{ap11})$	$-.65$	.17	.20	.72		
$\Re(S_{ap12})$	.20	.72	.65	$-.17$		
$\Im(S_{ap12})$	$-.72$	.20	$-.17$	$-.65$		
s_{ii}	1.5	1.5	1.4	1.4	0.01	0.01

Table 1: The vectors $\vec{v}_i$ and their associated singular value for the linearized one error box identification problem. Measured S-parameters at 10 GHz from the structures in fig. 4 were used. The identified exact solution is $Z_l = 51.7 + j7.6$ Ohm, $S_{ap11} = -0.01 - j0.01$ and $S_{ap12} = 0.98 - j0.02$, if $Z_s = 50$ Ohm.

3 A bidirectional search

The iterative solution of $\vec{f}(\vec{x}) = \vec{0}$ searches for all unknowns simultaniously and is a forward search method. Direct extraction, backward search, methods calculate unknown per unknown from selected measurements. A bidirectional search approach[Lin94] was implemented to exploit the sensitivity difference and to reduce the number of unknowns from $4M+2$ to 2. The line impedance Z_l is the ordinary optimization unknown, and the probe disturbance is extracted as follows: for every port x

1. calculate S_z and $S_{z,inv} = S_z(Z_l, Z_s)$ from Z_l, with $\vec{x} = [\Re(Z_l); \Im(Z_l)]$,
2. recover the probe response from the measurements S^{cal}_x using $S^{rec}_{xp} = S^{cal}_x \| S_{z,inv}$,
3. extract a better estimate with

$$S^{est}_{xp11} = (S^{rec}_{xp11} + S^{rec}_{xp22})/2 \qquad (6)$$
$$S^{est}_{xp12} = (S^{rec}_{xp12} + S^{rec}_{xp21})/2\,, \qquad (7)$$

4. calculate $S^{cir}_x = S^{est}_{xp} \| S_z$,
5. evaluate (4) and add the 8 results to $\vec{f}$.

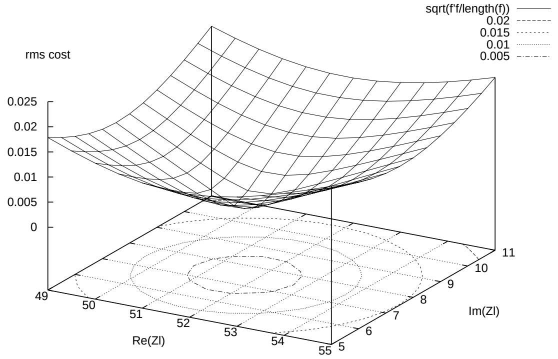

Figure 2: The rms cost of the bidirectional search method. A clear distinct minimum with equal sensitivity for the real and imaginary part is centered around the least squares solution $Z_l = 51.7 + j7.6$. The two error box experimental data is from the structures in fig. 4, at 10 GHz.

Repeating this procedure M times yields $8M$ equations. The condition of the linearized problem reduces to unity, indicating equal sensitivity for the real and imaginary part of Z_l. The internal condition is, however, unchanged and the probe related unknowns are still extracted with higher accuracy. The cost function for two trans-wafer error boxes, fig. 2, shows a well defined minimum. Robustness and convergence speed improve due to the efficient estimation (6) of the usually low probe reflections.

4 Experiment

The network analyzer was calibrated by a two port probe tip off-wafer LRM calibration on a coplanar alumina substrate. The thru loss and delay were estimated from the available lines. Multi-line TLR was used to calculate the LRM to TLR error boxes. A comparison of the line impedance phase, estimated from the new technique and the propagation constant method of [Mar91c], see fig. 3, validates the approach for low loss substrates.

The remaining difference may result from an inadequate error box model, here probably above 35 GHz, an increase in dielectric loss, assumed zero in [Mar91c], or non TE- or TM-behaviour, which invalidates (1) [Will93]. Also, using a non-zero length thru and probe tip loads in the off-wafer calibration introduces an error if the thru characteristic impedance differs from the load impedance.

The on-wafer calibration structures consist of 0.5 μm thick Al 15/11/183 μm, strip/slot/ground plane, coplanar lines of 100, 340, 1300 and 6300 μm long, separated by a 1 μm thick dielectricum from a 5 S/m Si lossy substrate. Multi-line TLR was performed to obtain the error box data. Figure 4 summarizes the results, which are consistent with [Glsn94]. Especially the low frequency RC behaviour, up to 1 GHz, and the high loss transition between the slow-wave and the dielectric quasi-TEM mode, at 3 GHz, is clearly visible.

The series and parallel loss was calculated from

$$\begin{aligned} \gamma &= \sqrt{(R+j\omega L)(G+j\omega C)} && (8)\\ &\approx \frac{R}{2\Re(Z_l)} + \frac{G\Re(Z_l)}{2} + j\omega\sqrt{LC} && (9) \end{aligned}$$

which holds if $\omega L \gg R$ and $\omega C \gg G$, since

$$\begin{aligned} Z_l &= \sqrt{\frac{R+j\omega L}{G+j\omega C}} && (10)\\ &\approx \sqrt{\frac{L}{C}}\left[1+j\left(\frac{G}{2\omega C}-\frac{R}{2\omega L}\right)\right] && (11) \end{aligned}$$

is then valid. The error in (9), for the here presented data, is below 1.5% above 1 GHz.

5 Conclusion

A robust line impedance identification method was presented. The method compares two calibrations and assumes that the difference is a symmetric error. Any non-symmetry is thus attributed to a reference impedance change. The method is reflection parameter based and avoids any transformation into chain or transmission parameters.

Acknowledgment

The author is supported by the Institute for the Promotion of Innovation by Science and Technology in Flanders (IWT). D. Schreurs is supported by the Fund for Scientific Research (FWO). D. Vanhoenacker, Université Catholique de Louvain, is acknowledged for making available the measurements used to develop the presented technique. The reported data is from a silicon wafer designed and processed by IMEC.

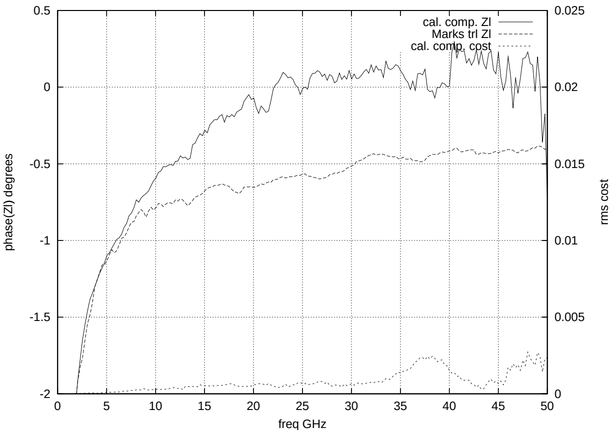

Figure 3: A comparison of the phase of the extracted line impedance using the new technique and the propagation constant method. The TLR standards consisted of 6 cpw lines, 50/25/200 μm strip/slot/ground plane wide and 197.4, 432.9, 870.9, 1736.8, 1736.8, 3383.1, 5080 μm long, fabricated on an alumina substrate. An initial LRM calibration was used as off-wafer reference.

References

[Car98] G. Carchon, D. Schreurs, S. Vandenberghe, B. Nauwelaers, W. De Raedt, “Compensating differences between measurement and calibration wafer in probe tip calibrations - deembedding of line parameters,” *1998 European Microwave Conference,* Amsterdam, October 1998, pp. 259–264.

[Col66] R. Collin, “Foundations for Microwave Engineering,” McGraw-Hill, New York, 1966.

[Glsn94] E. Grotelüschen, L.S. Dutta, S. Zaage, “Quasi-analytical Analysis of the Broadband Properties of Multiconductor Transmission Lines on Semiconducting Substrates,” *IEEE Transactions on Components, Packaging and Manufacturing Technology–Part B,* Vol. 17, No. 3, August 1994, pp. 376–382.

[Lin94] F. Lin, G. Kompa, “FET Model Parameter Extraction Based on Optimization With Multiplane Data-Fitting and Bidirectional Search–A New Concept,” *IEEE Transactions on Microwave Theory and Techniques,* Vol. 42, No. 7, July 1994, pp. 1114–1121.

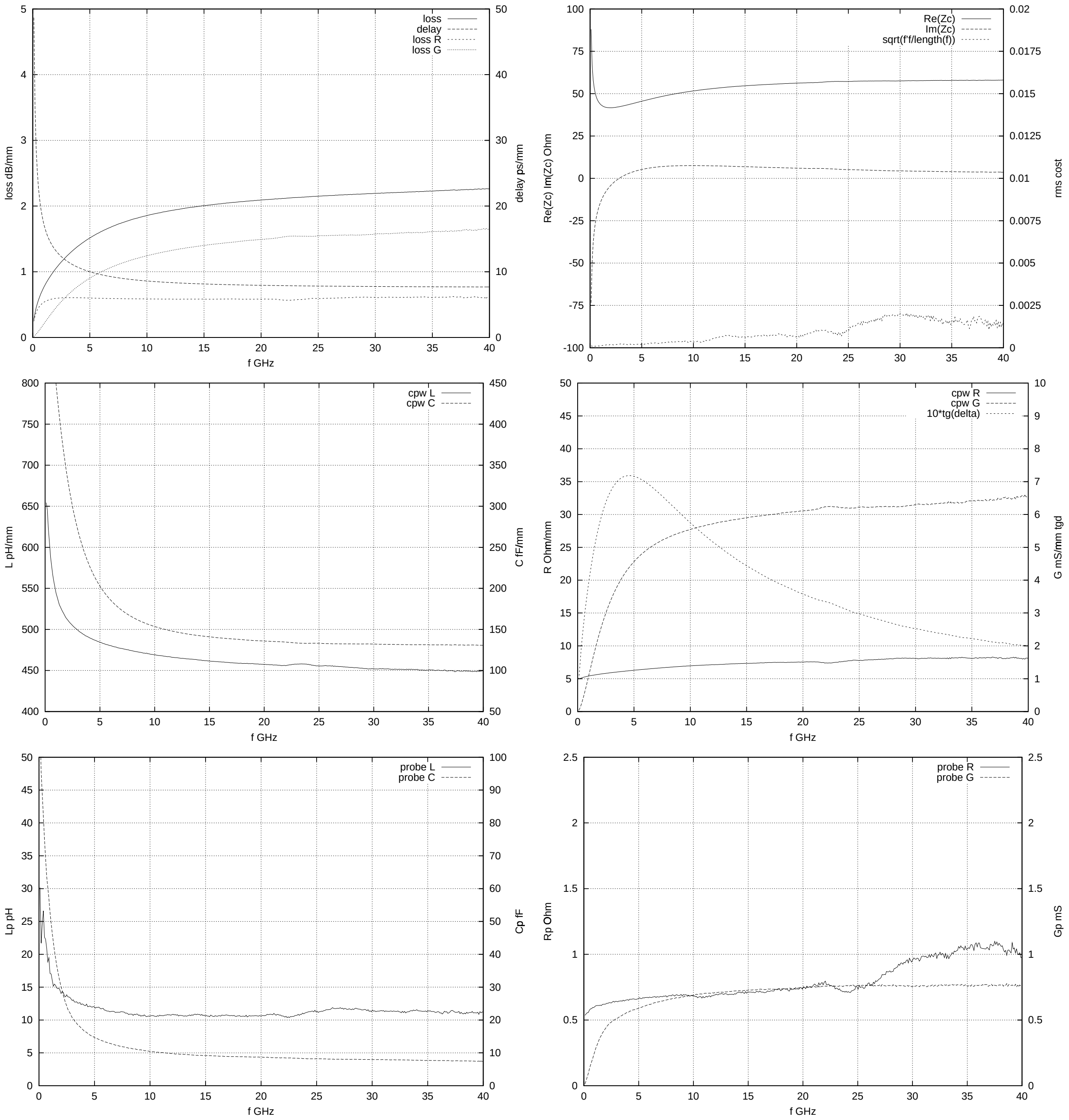

Figure 4: Top left: the line loss, delay, and the series and parallel loss calculated from the telegrapher's equation. Top right: the estimated line impedance and the error box fit cost. Center: the extracted line L, C and R, G,tgδ. Bottom: the total extracted probe L, C and R, G, averaged over error box a and b. All plots are for 0.5 μm thick Al 15/11/183 μm coplanar lines separated from a 5 S/m Si substrate by a 1 μm thick dielectricum. The lines were 100, 340, 1300 and 6300 μm long.

[Mar91c] R. Marks, D. Williams, "Characteristic Impedance Determination Using Propagation Constant Measurement," *IEEE Microwave and Guided Wave Letters,* Vol. 1, No. 6, June 1991, pp. 141–143.

[Will93] D. Williams, R. Marks, "Reciprocity Relations in Waveguide Junctions," *IEEE Transactions on Microwave Theory and Techniques,* Vol. 41, No. 6/7, June/July 1993, pp. 1105–1110.

[Will98] D. Williams, U. Arz, H. Grabinski, "Accurate Characteristic Impedance Measurement on Silicon," *IEEE MTT-S Digest,* 1998, pp. 1917–1920.